



# Tomography Simulation for the Profile Monitor in the ARIEL RIB Module

*Jensen Lawrence*

*TRIUMF*

**Abstract:** Throughout most of the ARIEL beamline, profile monitors are inserted into the beamline at an angle of  $45^\circ$  to the horizontal plane ( $x$ ). This means that two of the detector wires inside the profile monitor are aligned with the  $x$  and  $y$  axes, and the third is at an angle of  $45^\circ$  between the first two. However, in the RIB module, profile monitors must be inserted into the beamline at an angle of  $90^\circ$  relative to the horizontal plane. As a result, two of the detector wires inside the profile monitor are aligned at  $\pm 45^\circ$  relative to the horizontal plane, and the third is aligned with the horizontal plane. This report seeks to examine how this alternate orientation for the profile monitors affects the accuracy of beam profile reconstructions created using tomography techniques.

## Contents

<b>1</b>	<b>Introduction</b>	<b>2</b>
1.1	Profile Monitors in the RIB Module . . . . .	2
1.2	Method . . . . .	4
<b>2</b>	<b>Results and Comparison</b>	<b>5</b>
2.1	Elliptical Beam . . . . .	5
2.2	Quadratic Beam . . . . .	8
2.3	Cubic Beam . . . . .	11
2.4	Sinusoidal Beam . . . . .	14
2.5	General Comments . . . . .	17
2.6	Extensions . . . . .	17
<b>3</b>	<b>Modifying Profile Monitor Angles</b>	<b>18</b>
3.1	Elliptical Beam . . . . .	18
3.2	Quadratic Beam . . . . .	21
3.3	Cubic Beam . . . . .	24
3.4	Sinusoidal Beam . . . . .	27
<b>4</b>	<b>Conclusion</b>	<b>30</b>

# 1 Introduction

## 1.1 Profile Monitors in the RIB Module

In sections of the ARIEL beamline outside of the target hall, the beam profile monitors can be inserted into the beam at an angle of  $45^\circ$  relative to the horizontal plane ( $x$ ) (see Fig.1). This allows for the three detector wires inside the profile monitor to be oriented along the  $x$ ,  $y$  and  $45^\circ$  axes.

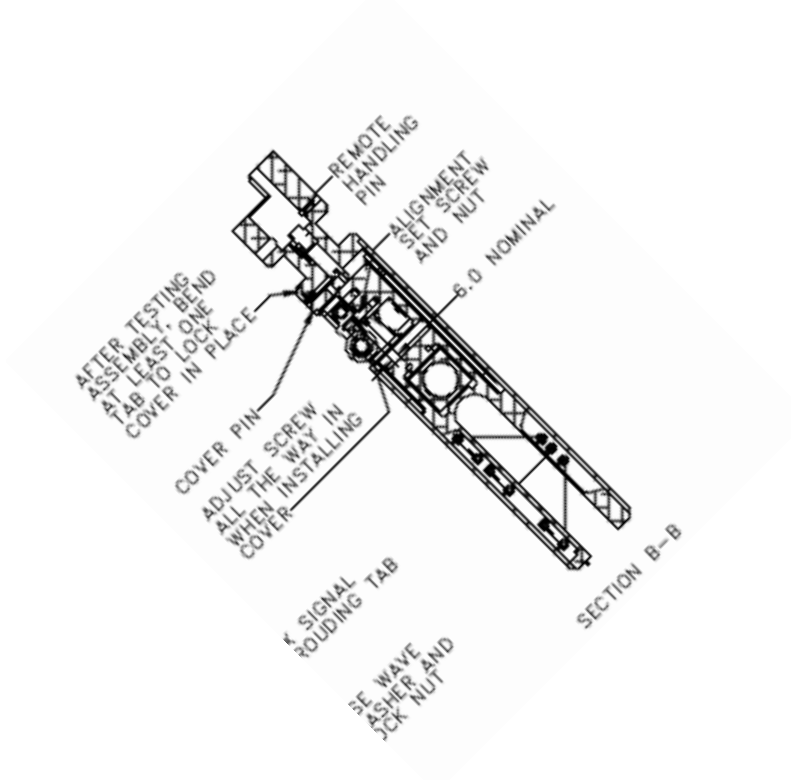


Figure 1: Layout of the Profile Monitor Installed at the ARIEL RIB Beamline Outside of the Target Hall. Inserted at  $45^\circ$  With Respect to the Horizontal Plane ( $x$ ).

This orientation is standard throughout the beam, and has been shown to produce excellent results<sup>1</sup>. Throughout this report, this orientation will be referred to as the **standard orientation**.

However, in the RIB module in the ARIEL pre-separator, space around the beamline is restricted<sup>2</sup>. As a result, profile monitors cannot be placed into the beam in their standard orientation. Rather, the profile monitor is inserted into the beamline at  $90^\circ$  with respect to the horizontal plane ( $x$ ) (see Fig.2). This means that the detector wires are oriented along the  $x$ ,  $-45^\circ$ , and  $45^\circ$  axes.

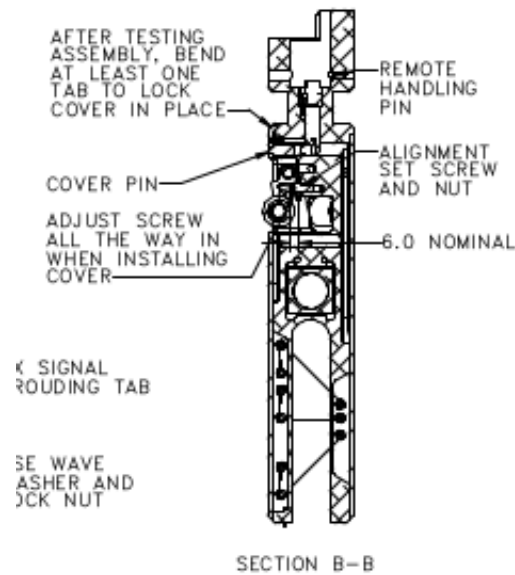


Figure 2: Layout of the Profile Monitor Installed at the ARIEL RIB Beamline Inside the Target Hall. Inserted at  $90^\circ$  With Respect to the Horizontal Plane ( $x$ ).

Throughout this report, this orientation will be referred to as the **alternate orientation**.

Due to this alternate orientation, the beam will be measured differently in the RIB module than elsewhere in the beamline, as different parts of the beam are sampled. It is unknown if or how this will affect the real-space reconstructions of the beam profile created using tomography methods. We turn to simulation in order to address this problem. Specifically, we will examine what the effects of this alternate orientation are (if there are any), the significance of these effects, and how they can be addressed.

Along with investigating how elliptical beams are reconstructed, we also investigate how beams with other shapes, such as quadratic or cubic, are reconstructed in order to account for potential aberrations in the beam during experimentation.

## 1.2 Method

The first step in determining the effect of the alternate orientation was obtaining simulation data. For this investigation, 100 000 particles of  $^{133}\text{Cs}^{1+}$  at 30 KeV were simulated at the location of COL8A<sup>2</sup>. This simulated beam serves as the template for other simulated beams used in this investigation, and will be referred to from now on as simply the elliptical beam.

The next step was to write a program which performs all that is required by this investigation. To fill this need, a multi-purpose Python script was written. The first function of this program is that it can receive the simulation data as a user input and then plot the data as a contour plot. This is to produce a profile of the simulated beam, which can later be compared to the profiles of the reconstructed beams. The user is also capable of creating new beam profiles, such as the modified profiles seen later in this report, by changing how the program processes the simulation data. Next, the program uses the simulation data to construct data “measured” from additional axis at  $45^\circ$  in the case of the standard profile monitor, or from two additional axes at  $\pm 45^\circ$  in the case of the RIB module profile monitor. This was done by means of a rotation matrix. After this, the program determines the transfer matrices corresponding to each axis. Finally, the program writes the three axes of “measured” data, either  $(x, 45^\circ, y)$  in the case of the standard orientation or  $(-45^\circ, x, 45^\circ)$  in the case of the alternate orientation, along with the transfer matrices, to an output file. This file contains data which appears as if it was measured in an experiment by a profile monitor.

The final step was to analyze this “measured” data. Using Ment, a program which creates tomography reconstruction data from beam profile data, the “measured” data can be used to try and reconstruct the initial beam profile. The resulting beam profile, in the form of a contour plot, is then compared to the initial contour plot which were constructed directly from the simulation data. Through this comparison, it can be determined how accurately beam profiles can be reconstructed using tomography from data collected by a profile monitor with a given orientation.

The effect that the alternate orientation has on beam reconstruction can then be determined by comparing the alternate orientation reconstructed profile to the standard orientation reconstructed profile and to the simulated profile.

For a thorough investigation, the reconstruction of the elliptical beam will be performed, as well as the reconstruction of beams which have been modified to have quadratic, cubic, and sinusoidal profiles. This way the effect of beam aberrations can be tested as well, since beams are not necessarily elliptical in experiment.

## 2 Results and Comparison

### 2.1 Elliptical Beam

The figure below is a contour plot of the elliptical beam profile. They were constructed by plotting the elliptical beam data, and have not been processed in any way. The figure serves as the theoretical comparison to the two reconstructed beam profiles on the following page.

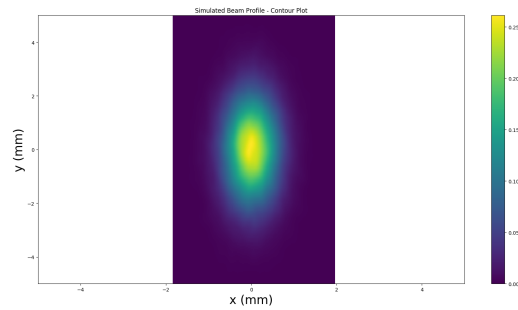


*Figure 3: A Contour Plot of the Simulated Elliptical Beam Profile.*

Now, we examine how this elliptical beam profile was reconstructed by using the standard and alternate orientations.

To simulate a measurement of an elliptical beam with a standard orientation profile monitor, an axis at  $45^\circ$  with respect to the  $x$  axis was constructed artificially by rotating the  $x$  measurements of the simulated elliptical beam. Then, a data file was created which contained the values measured along this new  $45^\circ$  axis, as well as the simulated values measured along the  $x$  and  $y$  axes. Finally, this data was processed using tomography, resulting in the following reconstruction:

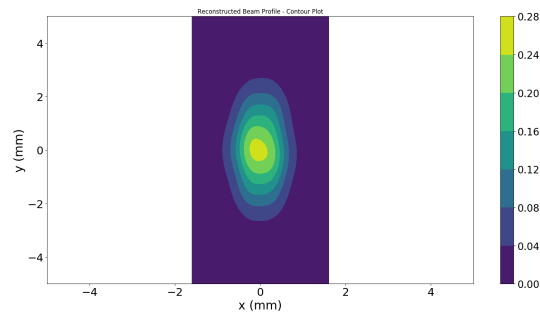


*Figure 4:* A Contour Plot of the Elliptical Beam Profile Reconstructed Using Tomography Based On Data Simulated to Have Been Collected by a Profile Monitor With the Standard Orientation

To simulate a measurement of an elliptical beam with an alternate orientation profile monitor, two axes at  $\pm 45^\circ$  with respect to the  $x$  axis were constructed artificially by rotating the  $x$  measurements of the simulated elliptical beam. Then, a data file was created which contained the values measured along these new  $\pm 45^\circ$  axis, as well as the simulated values measured along the  $x$  axis. Finally, this data was processed using tomography, resulting in the following reconstruction:

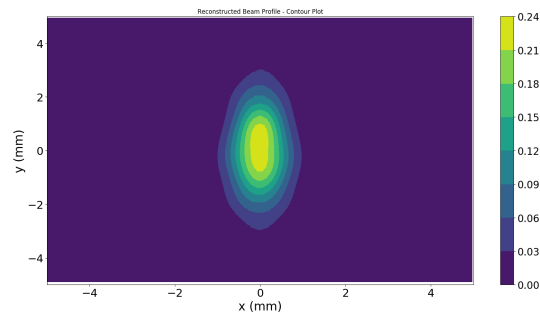


*Figure 5:* A Contour Plot of the Elliptical Beam Profile Reconstructed Using Tomography Based On Data Simulated to Have Been Collected by a Profile Monitor With the Alternate Orientation

We see that the standard orientation reconstruction in Figure 4 is a more accurate reconstruction than the alternate orientation reconstruction in Figure 5, although only marginally so. We see that the simulated beam profile in Figure 3 has an elliptical shape, smooth edges, and a maximum intensity of 0.26. Similarly, we see that the standard orientation reconstruction in Figure 4 has a shape very close to elliptical, mostly smooth edges, and a maximum intensity of 0.28. The alternate orientation reconstruction deviates more as its shape is less elliptical and there are some clearly defined edges along the beam profile. Furthermore, the maximum intensity is 0.24 and the contours are more vertically stretched than in the simulation profile or the standard orientation reconstruction. Based on these reconstructions, we can conclude that the standard orientation is more effective at reconstructing elliptical beams than the alternate orientation.

However, it is worth noting that the general properties of the simulated beam can still be determined using the alternate orientation reconstruction. The reconstructed maximum intensity value is quite close to the true maximum intensity value, and it is obvious that the beam is elliptical, despite the defined edges. So, although the alternate orientation is not as effective as the standard orientation for elliptical beams, it still provides a result that is clearly similar to the simulated beam profile.



## 2.2 Quadratic Beam

The figure below is a contour plot of the quadratic beam profile. To construct a quadratic beam, the  $x$  values of the elliptical beam data was modified using the following formula:

$$x_{quad} = \frac{1}{10}y^2 - x$$

The new  $x$  values, along with the original  $y$  values, were then plotted. The figure serves as the theoretical comparison to the two reconstructed beam profiles on the following page.

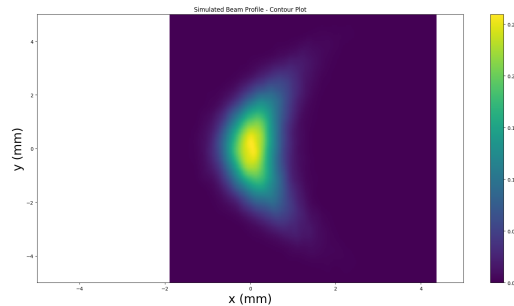


Figure 6: A Contour Plot of the Simulated Quadratic Beam Profile.

Now, we examine how this quadratic beam profile was reconstructed by using the standard and alternate orientations.

To simulate a measurement of a quadratic beam with a standard orientation profile monitor, an axis at  $45^\circ$  with respect to the  $x$  axis was constructed artificially by rotating the  $x$  measurements of the simulated quadratic beam from the previous page. Then, a data file was created which contained the values measured along this new  $45^\circ$  axis, as well as the simulated values measured along the  $x$  and  $y$  axes. Finally, this data was processed using tomography, resulting in the following reconstruction:

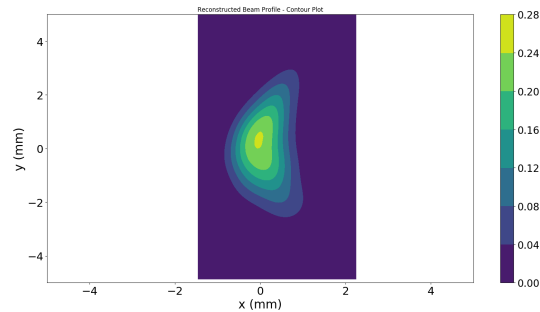


Figure 7: A Contour Plot of the Quadratic Beam Profile Reconstructed Using Tomography Based On Data Simulated to Have Been Collected by a Profile Monitor With the Standard Orientation

To simulate a measurement of an quadratic beam with an alternate orientation profile monitor, two axes at  $\pm 45^\circ$  with respect to the  $x$  axis were constructed artificially by rotating the  $x$  measurements of the simulated quadratic beam from the previous page. Then, a data file was created which contained the values measured along these new  $\pm 45^\circ$  axis, as well as the simulated values measured along the  $x$  axis. Finally, this data was processed using tomography, resulting in the following reconstruction:

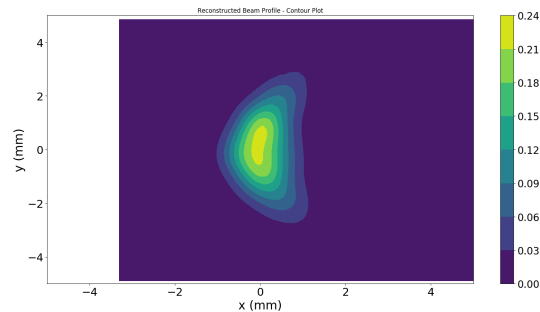


Figure 8: A Contour Plot of the Quadratic Beam Profile Reconstructed Using Tomography Based On Data Simulated to Have Been Collected by a Profile Monitor With the Alternate Orientation

We see that the alternate orientation reconstruction in Figure 8 is actually a more accurate reconstruction than the standard orientation reconstruction in Figure 7, indicating that for a quadratically skewed beam there is no risk of poor reconstruction when compared to the standard reconstruction that would be seen elsewhere in the beamline. This also indicates that some revisions may need to be made either to the standard orientation or how data collected from the standard orientation is processed, however that is not the focus of this report. Consider Figure 6, the simulated beam profile. It exhibits symmetry about the  $x$  axis, tapers rapidly to its tips, and has a maximum intensity value of around 0.26. The RIB module profile monitor reconstruction in Figure 8 exhibits the same symmetry about the  $x$  axis and has a maximum intensity value of 0.24. However, the rapid taper is almost entirely absent, with the right edge instead being nearly a straight line. The standard profile monitor reconstruction in Figure 7 has different problems than the RIB module profile monitor reconstruction. Figure 7 is more similar to Figure 6 in that there is a little more of a taper present, however, there is a noticeable asymmetry about the  $x$  axis, which is unlike Figure 6.

Overall, since the alternate method produces a more accurate reconstruction of the quadratic beam, there should not be any major problems experienced when reconstructing quadratic beams in the RIB module.

## 2.3 Cubic Beam

The figure below is a contour plot of the profile of the cubic beam. To construct a cubic beam, the  $x$  values of the elliptical beam data was modified using the following formula:

$$x_{cubic} = \frac{1}{15}y^3 - x$$

The new  $x$  values, along with the original  $y$  values, were then plotted. The figure serves as the theoretical comparison to the two reconstructed beam profiles on the following page.

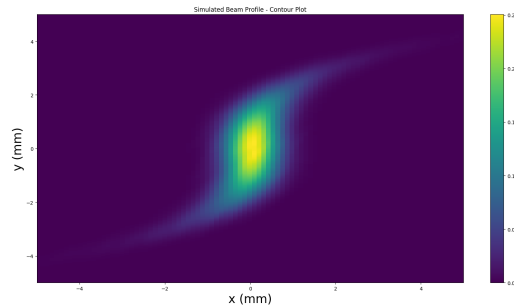
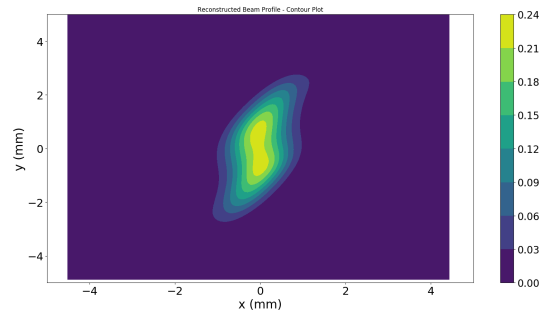


Figure 9: A Contour Plot of the Simulated Cubic Beam Profile.

Now, we examine how this cubic beam profile was reconstructed by using the standard and alternate orientations.

To simulate a measurement of a cubic beam with a standard orientation profile monitor, an axis at  $45^\circ$  with respect to the  $x$  axis was constructed artificially by rotating the  $x$  measurements of the simulated cubic beam from the previous page. Then, a data file was created which contained the values measured along this new  $45^\circ$  axis, as well as the simulated values measured along the  $x$  and  $y$  axes. Finally, this data was processed using tomography, resulting in the following reconstruction:



*Figure 10: A Contour Plot of the Cubic Beam Profile Reconstructed Using Tomography Based On Data Simulated to Have Been Collected by a Profile Monitor With the Standard Orientation*

To simulate a measurement of an cubic beam with an alternate orientation profile monitor, two axes at  $\pm 45^\circ$  with respect to the  $x$  axis were constructed artificially by rotating the  $x$  measurements of the simulated cubic beam from the previous page. Then, a data file was created which contained the values measured along these new  $\pm 45^\circ$  axis, as well as the simulated values measured along the  $x$  axis. Finally, this data was processed using tomography, resulting in the following reconstruction:

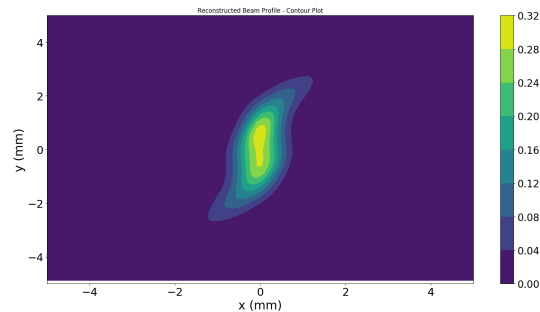


*Figure 11: A Contour Plot of the Cubic Beam Profile Reconstructed Using Tomography Based On Data Simulated to Have Been Collected by a Profile Monitor With the Alternate Orientation*

We see that the alternate orientation reconstruction in Figure 11 is actually a more accurate reconstruction than the standard orientation reconstruction in Figure 10, indicating that for a cubically skewed beam there is no risk of poor reconstruction when compared to the standard reconstruction that would be seen elsewhere in the beamline. This also indicates that some revisions may need to be made either to the standard orientation or how data collected from the standard orientation is processed, however that is not the focus of this report. Consider Figure 9, the simulated beam profile. It exhibits antisymmetry about the  $x$  and  $y$  axes, has a constant width in its central section, then tapers to two long tails which protrude in opposite directions. Its maximum intensity value is around 0.25, and the area of maximum intensity is an ellipse in the centre of the beam. The alternate orientation reconstruction in Figure 11 exhibits the same antisymmetry about both axes, has a constant width in its central section, and has some tails which do taper off in opposite directions (although they are shorter). The RIB module did not reconstruct the intensity of the beam properly, as is shown by the non-elliptical area of maximum intensity, and that the maximum intensity value is 0.32, which is much higher than the true value. The standard orientation reconstruction in Figure 11 has different problems than the RIB module profile monitor reconstruction. It too exhibits a roughly antisymmetric shape about both axes, and has a maximum intensity value of 0.24. However, the shape of the maximum intensity region is not elliptical, and the shape of the beam overall differs greatly from the true profile. This reconstruction has nearly constant width throughout, and there is very little sign of any taper or the tails seen in the true profile.

Overall, since the alternate method produces a more accurate reconstruction of the quadratic beam, there should not be any major problems experienced when reconstructing cubic beams in the RIB module.

## 2.4 Sinusoidal Beam

The figure below is a contour plot of the profile of the sinusoidal beam. To construct a sinusoidal beam, the  $x$  values of the elliptical beam data was modified using the following formula:

$$y_{sin} = \sin(2x) + \frac{y}{10}$$

The new  $y$  values, along with the original  $x$  values, were then plotted. The figures serve as the theoretical comparison to the two reconstructed beam profiles on the following page.

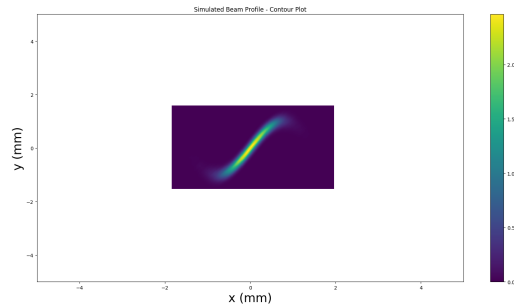
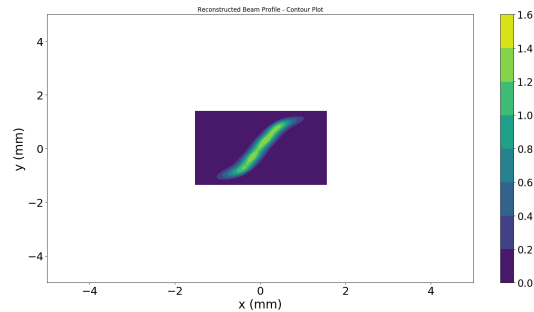


Figure 12: A Contour Plot of the Simulated Sinusoidal Beam Profile.

Now, we examine how this sinusoidal beam profile was reconstructed by using the standard and alternate orientations.

To simulate a measurement of a sinusoidal beam with a standard orientation profile monitor, an axis at  $45^\circ$  with respect to the  $x$  axis was constructed artificially by rotating the  $x$  measurements of the simulated sinusoidal beam from the previous page. Then, a data file was created which contained the values measured along this new  $45^\circ$  axis, as well as the simulated values measured along the  $x$  and  $y$  axes. Finally, this data was processed using tomography, resulting in the following reconstruction:



*Figure 13: A Contour Plot of the Sinusoidal Beam Profile Reconstructed Using Tomography Based On Data Simulated to Have Been Collected by a Profile Monitor With the Standard Orientation*

To simulate a measurement of an sinusoidal beam with an alternate orientation profile monitor, two axes at  $\pm 45^\circ$  with respect to the  $x$  axis were constructed artificially by rotating the  $x$  measurements of the simulated sinusoidal beam from the previous page. Then, a data file was created which contained the values measured along these new  $\pm 45^\circ$  axis, as well as the simulated values measured along the  $x$  axis. Finally, this data was processed using tomography, resulting in the following reconstruction:

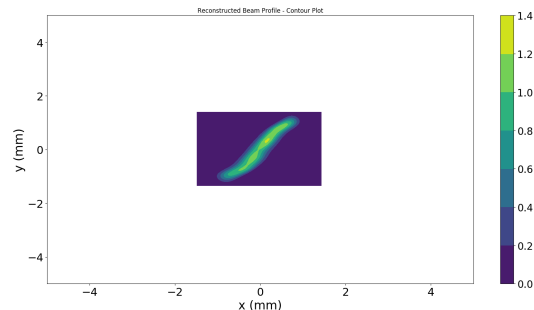


*Figure 14: A Contour Plot of the Sinusoidal Beam Profile Reconstructed Using Tomography Based On Data Simulated to Have Been Collected by a Profile Monitor With the Alternate Orientation*



We see that the standard orientation reconstruction in Figure 13 is a more accurate reconstruction than the alternate orientation reconstruction in Figure 14. Consider Figure 12, the simulated beam profile. The intensity is greatest in a central line, the beam is slanted diagonally, and the ends curve over. It has a maximum intensity value of around 2.5. The standard orientation reconstruction in Figure 13 mostly agrees with this result, having a very similar shape and a central line of maximum intensity. The alternate orientation reconstruction in Figure 14 has approximately the correct shape, however it is much thicker in the middle, has a central bulge not present in the true profile, and the curve at the ends of the profile is much less evident. As well, the area of maximum intensity is broken into multiple parts rather than being a straight line. Both reconstructions fail to accurately represent the maximum beam intensity, with values of 1.6 and 1.4 respectively. Based on these reconstructions, we can conclude that the standard orientation is more effective at reconstructing sinusoidal beams than the alternate orientation. It is worth noting that this is not necessarily a very realistic beam shape, and was mostly included to push the limits of the reconstruction.

## 2.5 General Comments

Overall, it appears that the RIB module profile monitors tend to have problems accurately measuring the intensity and intensity gradient of the beam. For each case, it measured a maximum intensity value of 0.24, 0.24, 0.32, and 1.4, respectively. This is in contrast to the simulated values of 0.26, 0.26, 0.25, and 2.5. So for the elliptical and quadratic beams it slightly undermeasured, for the cubic beam it greatly overmeasured, and for the sinusoidal beam it greatly undermeasured. In the case of the elliptical, cubic, and sinusoidal beams, it also had problems accurately reconstructing the proper shape and contour lines for each region of intensity.

There also seem to be some challenges when it comes to reconstructing fainter areas of a beam. For example, the tails on the quadratic and cubic beams, as well as the end curves on the sinusoidal beam, were essentially ignored by the reconstruction. Although the central part of the beam is the most important, missing details such as these could still be detrimental to experimentation.

Thankfully, the RIB module profile monitor seems to be able to reconstruct an elliptical beam profile in a satisfactory manner (although not as good as the standard profile monitor). This reconstruction is quite important since the ideal beam shape, and hopefully the beam shape which will be seen most frequently in the beamline, is elliptical.

Interestingly, this investigation has also revealed flaws with the standard profile monitor's reconstruction capabilities, even though they were initially only used for comparison purposes. Like the RIB module profile monitor, the standard profile monitors seems to ignore edge details such as tails. Unlike the RIB module profile monitor, the standard profile monitor seems to have issues accurately reconstructing beams with symmetry about only one axis, as was seen with the asymmetry in the quadratic beam reconstruction.

## 2.6 Extensions

One may wonder whether changing the design of the RIB module profile monitor would result in more favourable outcomes and more accurate measurements. In the following section, we investigate the effect of changing the angles of the RIB module profile monitor detectors, varying the values from  $\pm 30^\circ$  to  $\pm 60^\circ$  by increments of  $\pm 5^\circ$ . Note that  $\pm 45^\circ$  is not included, since the results for this angle have already been analyzed in this section. Angles from  $\pm 5^\circ$  to  $\pm 85^\circ$  were initially considered, but angles outside the  $\pm 30^\circ$  to  $\pm 60^\circ$  were discarded when it became clear that reconstructions were highly inaccurate outside of that range.

### 3 Modifying Profile Monitor Angles

#### 3.1 Elliptical Beam

We now examine how the alternate orientation reconstructs an elliptical beam using different configurations of the angled detectors inside the monitor.

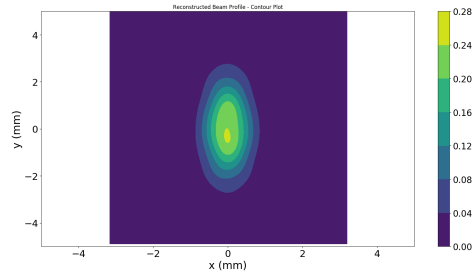


Figure 15: Contour Plot Constructed by Simulating Data Collected from an Elliptical Beam with  $\pm 30^\circ$  Profile Monitor Detectors.

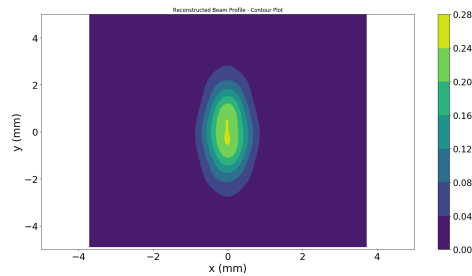


Figure 16: Contour Plot Constructed by Simulating Data Collected from an Elliptical Beam with  $\pm 35^\circ$  Profile Monitor Detectors.

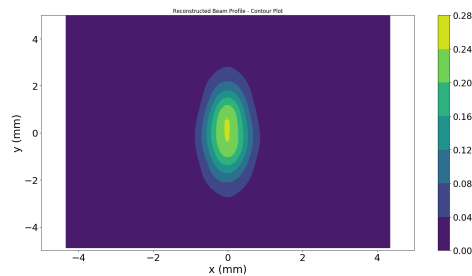


Figure 17: Contour Plot Constructed by Simulating Data Collected from an Elliptical Beam with  $\pm 40^\circ$  Profile Monitor Detectors.

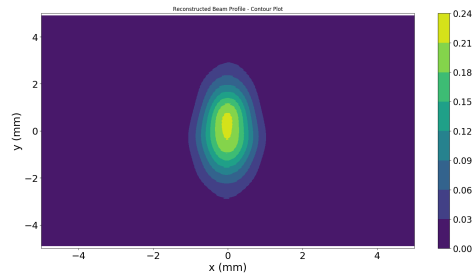


Figure 18: Contour Plot Constructed by Simulating Data Collected from an Elliptical Beam with  $\pm 50^\circ$  Profile Monitor Detectors.

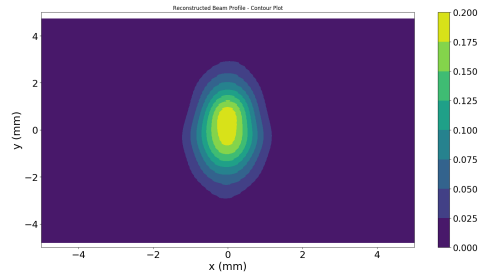


Figure 19: Contour Plot Constructed by Simulating Data Collected from an Elliptical Beam with  $\pm 55^\circ$  Profile Monitor Detectors.

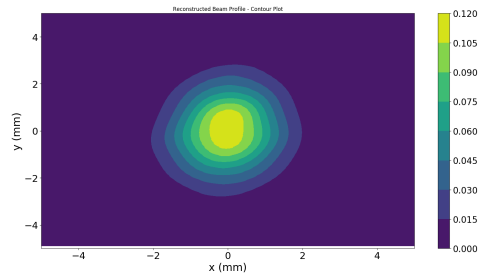


Figure 20: Contour Plot Constructed by Simulating Data Collected from an Elliptical Beam with  $\pm 60^\circ$  Profile Monitor Detectors.

Figure 15 was discarded as a possibility due to its inaccurate reconstruction of the central part of the beam. Figures 18, 19, and 20 were discarded as possibilities because it is clear that they do not reconstruct the overall shape of the beam properly, and Figures 22 and 23 greatly undermeasure the maximum intensity value. This leaves Figures 16 and 17, corresponding to axis angles of  $\pm 35^\circ$  and  $\pm 40^\circ$ . Both appear to have the correct elliptical shape overall, which is a positive start. Closer examination of Figure 16 reveals a poorly-formed central region, so this option is now discarded, leaving  $\pm 40^\circ$  as an option. Although this is a somewhat acceptable reconstruction, comparing it to the results in Figure 5 from  $\pm 45^\circ$  show that in reference to the simulated results in Figure 3,  $\pm 45^\circ$  axes do a better job at reconstructing the beam profile than  $\pm 40^\circ$  axes. Thus, none of the alternate angles do a better job at reconstructing an elliptical beam.

### 3.2 Quadratic Beam

We now examine how the alternate orientation reconstructs a quadratic beam using different configurations of the angled detectors inside the monitor.

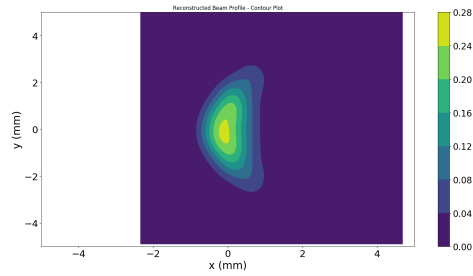


Figure 21: Contour Plot Constructed by Simulating Data Collected from an Quadratic Beam with  $\pm 30^\circ$  Profile Monitor Detectors.

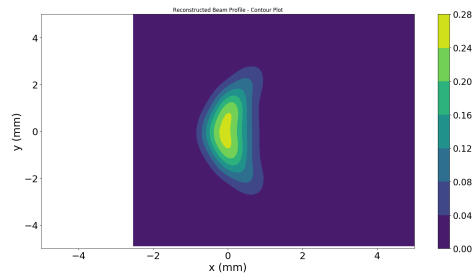


Figure 22: Contour Plot Constructed by Simulating Data Collected from an Quadratic Beam with  $\pm 35^\circ$  Profile Monitor Detectors.

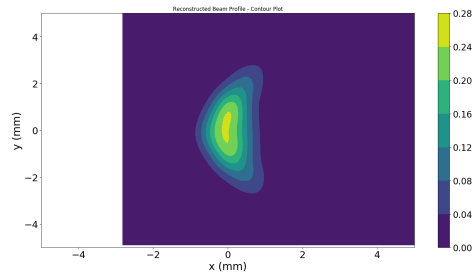


Figure 23: Contour Plot Constructed by Simulating Data Collected from an Quadratic Beam with  $\pm 40^\circ$  Profile Monitor Detectors.

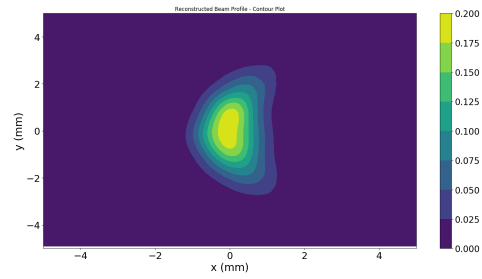


Figure 24: Contour Plot Constructed by Simulating Data Collected from an Quadratic Beam with  $\pm 50^\circ$  Profile Monitor Detectors.

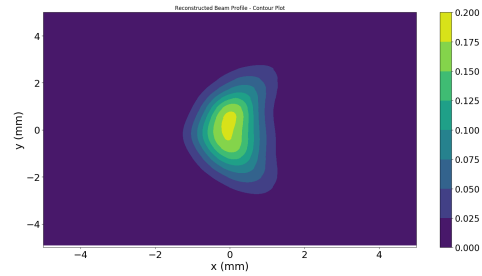


Figure 25: Contour Plot Constructed by Simulating Data Collected from an Quadratic Beam with  $\pm 55^\circ$  Profile Monitor Detectors.

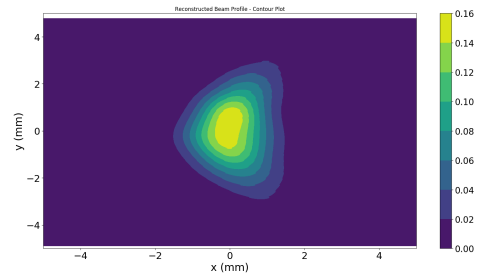


Figure 26: Contour Plot Constructed by Simulating Data Collected from an Quadratic Beam with  $\pm 60^\circ$  Profile Monitor Detectors.

Figure 21 was discarded as a possibility due to its inaccurate area of maximum intensity. Figures 24, 25, and 26 were discarded as possibilities because it is clear that they do not reconstruct the overall shape of the beam properly, and they all greatly undermeasure the maximum intensity value. This leaves Figures 22 and 23, corresponding to axis angles of  $\pm 35^\circ$  and  $\pm 40^\circ$ . Both are close to the results seen in Figure 6, which is the simulated beam profile. In fact, based on overall beam shape and the shape of the area of maximum intensity, it appears that for a quadratic beam, axis angles of  $\pm 35^\circ$  are best for reconstruction purposes. This is surprising, given that axis angles of  $\pm 35^\circ$  do not perform as well in other scenarios. However, changing the angles of the detectors to account for one edge case is illogical, meaning  $\pm 45^\circ$  is still the best choice.



### 3.3 Cubic Beam

We now examine how the alternate orientation reconstructs a cubic beam using different configurations of the angled detectors inside the monitor.

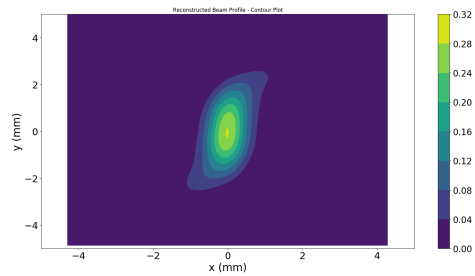


Figure 27: Contour Plot Constructed by Simulating Data Collected from an Cubic Beam with  $\pm 30^\circ$  Profile Monitor Detectors.

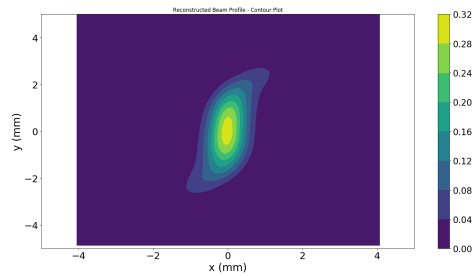


Figure 28: Contour Plot Constructed by Simulating Data Collected from an Cubic Beam with  $\pm 35^\circ$  Profile Monitor Detectors.

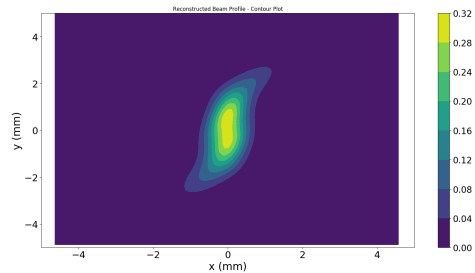


Figure 29: Contour Plot Constructed by Simulating Data Collected from an Cubic Beam with  $\pm 40^\circ$  Profile Monitor Detectors.

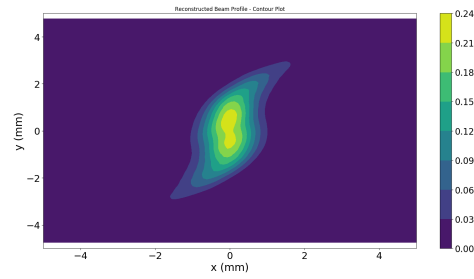


Figure 30: Contour Plot Constructed by Simulating Data Collected from an Cubic Beam with  $\pm 50^\circ$  Profile Monitor Detectors.

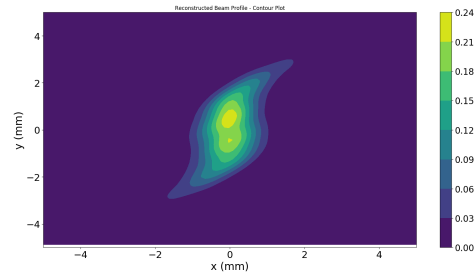


Figure 31: Contour Plot Constructed by Simulating Data Collected from an Cubic Beam with  $\pm 55^\circ$  Profile Monitor Detectors.

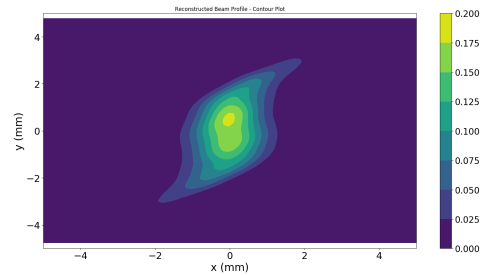


Figure 32: Contour Plot Constructed by Simulating Data Collected from an Cubic Beam with  $\pm 60^\circ$  Profile Monitor Detectors.

Figures 27 and 28 were discarded as possibilities due to the lack of extended tails, indicating they do not accurately reconstruct the beam. Figures 31 and 32 were discarded as possibilities because it is clear that they do not reconstruct the overall shape of the beam properly, and Figure 32 undermeasures the maximum intensity value. This leaves Figures 29 and 30, corresponding to axis angles of  $\pm 40^\circ$  and  $\pm 50^\circ$ . Figure 29 appears promising at first, however closer examination shows that its tails are not as pronounced as those in Figure 11, the  $\pm 45^\circ$  axis reconstruction. This means that  $\pm 40^\circ$  provide a less detailed reconstruction of the cubic beam. Figure 30 demonstrates the tails more prominently, however, the shape of the rest of the beam, especially the central area, is quite dissimilar to the simulated beam profile. Thus, none of the alternate angles do a better job at reconstructing a cubic beam.

### 3.4 Sinusoidal Beam

We now examine how the alternate orientation reconstructs a sinusoidal beam using different configurations of the angled detectors inside the monitor.

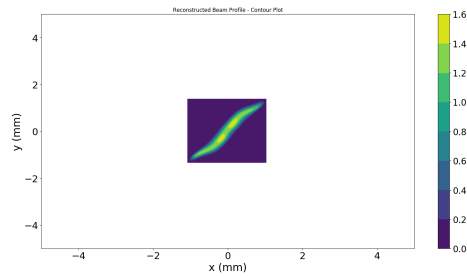


Figure 33: Contour Plot Constructed by Simulating Data Collected from an Sinusoidal Beam with  $\pm 30^\circ$  Profile Monitor Detectors.

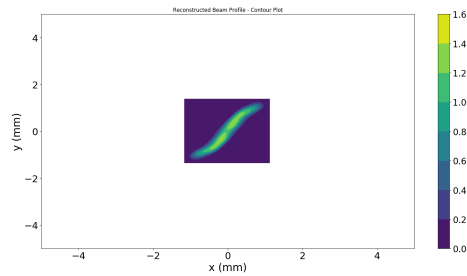


Figure 34: Contour Plot Constructed by Simulating Data Collected from an Sinusoidal Beam with  $\pm 35^\circ$  Profile Monitor Detectors.

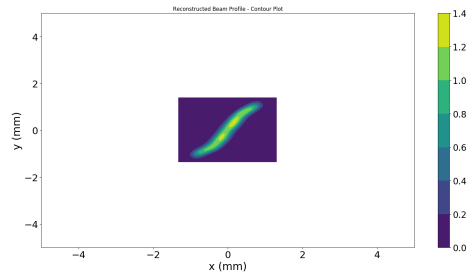


Figure 35: Contour Plot Constructed by Simulating Data Collected from an Sinusoidal Beam with  $\pm 40^\circ$  Profile Monitor Detectors.

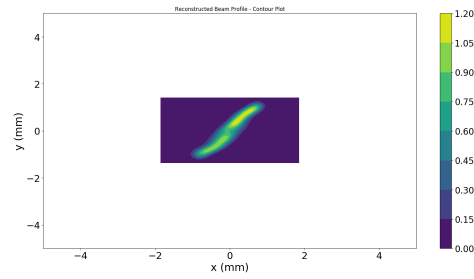


Figure 36: Contour Plot Constructed by Simulating Data Collected from an Sinusoidal Beam with  $\pm 50^\circ$  Profile Monitor Detectors.

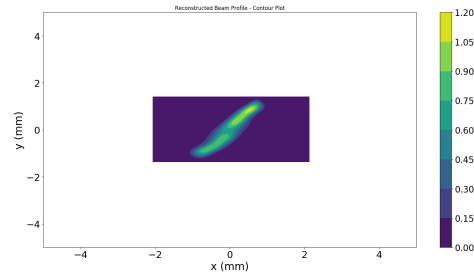


Figure 37: Contour Plot Constructed by Simulating Data Collected from an Sinusoidal Beam with  $\pm 55^\circ$  Profile Monitor Detectors.

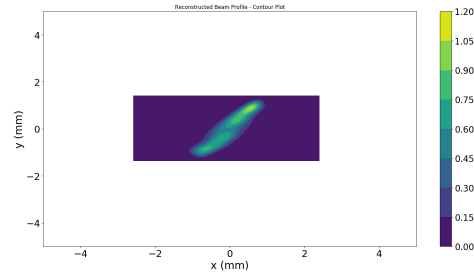


Figure 38: Contour Plot Constructed by Simulating Data Collected from an Sinusoidal Beam with  $\pm 60^\circ$  Profile Monitor Detectors.

None of Figures 33-38 are possibilities for a better reconstruction of the sinusoidal beam profile. They all demonstrate problems seen with the  $\pm 45^\circ$  axes but to a greater extent, such as the central bulge, the areas of maximum intensity not connecting, and a lack of curving at the ends of the beams. Thus, the  $\pm 45^\circ$  axes remain the best option, and none of the alternate angles do a better job at reconstructing a sinusoidal beam.

## 4 Conclusion

This investigation yielded multiple important results. First, we see that for elliptical and sinusoidal beams, the standard orientation is more effective at reconstructing the beam profile than the alternate orientation. This indicates that some improvement needs to be made upon the alternate orientation. However, when changes were implemented by altering the angles of the detector wires in the alternate orientation, the reconstructions were even worse than before. As well, the alternate orientation still reconstructs the elliptical beam in a fairly accurate manner, and a sinusoidal beam is an unlikely kind of aberration. Thus, the only changes which could be made to potentially improve the outcome is modifying the reconstruction software itself in some way to account for the effects of the alternate orientation.

For quadratic and cubic beams, the alternate orientation produces more accurate reconstructions than the standard orientation. This, when combined with the moderate success of the elliptical beam reconstruction, indicates that the alternate orientation is fairly accurate up to third-order aberrations. Furthermore, based on the ineffectiveness of altering the detector angles, we can conclude that no changes need to be made to the design of the profile monitor in the RIB module.

A potential extension in the future may be modifying the tomography software to try to account for the effects of the alternate orientation, and perhaps to reconstruct quadratic and cubic beams with the standard orientation more accurately.

## Appendix

**ARIEL:** Advanced Rare IsotopE Laboratory

**COL:** Collimator

**RIB:** Radioactive Ion Beam



## References

- [1] S. Saminathan, F. Ames, R. Baartman, M. Marchetto, O. Layley, and A. Mahon. “Tomography reconstruction of beams extracted from an ion source.” *Rev. Sci. Instrum.* 90, 123302 (2019).
- [2] S. Saminathan and R. Baartman. “ARIEL Pre-separator.” Technical Report TRI-DN-16-07, TRIUMF, 2016.